Contents list available at IJRED website

International Journal of Renewable Energy Development

Journal homepage: https://ijred.undip.ac.id

Research Article

Design and control of a hybrid water pumping system using energy management for sustainable agricultural irrigation: A case study of the Sidi Bouzid region in Tunisia

Akram Amri*, Intissar Moussa, Adel Khedher

LATIS (Laboratory of advanced Technology and Intelligent Systems), National Engineering School of Sousse, University of Sousse, Sousse, 4002,Tunisia

Abstract. In this study, a renewable energy-powered Hybrid Water Pumping System (HWPS) is proposed for agricultural irrigation, designed to operate without reliance on battery storage. The system is adapted to the local climatic characteristics of the Sidi Bouzid region in Tunisia and is intended to regulate and coordinate water flow to effectively meet crop irrigation requirements. Hence, the system comprises three principal subsystems: A Wind Turbine (WT) driving a Doubly-Fed Induction Generator (DFIG) connected to the grid via rotor-side and grid-side converters; a Photovoltaic (PV) module integrated via a DC/DC boost converter; and a water pumping unit, consisting of an Induction Machine (IM) coupled to a centrifugal pump. The mathematical models of each subsystem were developed, and a control algorithms suite was implemented to enhance overall performance and energy efficiency. Maximum Power Point Tracking (MPPT) techniques were employed to optimize the energy harvested from renewable sources. A non-linear Sliding Mode Control (SMC) strategy was implemented to manage the DFIG power output, while Input-Output Feedback Linearization (IOFL) was applied to control the IM via a Voltage Source Inverter (VSI).Since the system operates without battery storage, a dynamic Energy Management System (EMS) is investigated to ensure optimal energy distribution, prioritizing solar energy during peak sunlight hours and transitioning to wind energy when solar availability declines. Simulation results validate the system's effectiveness and demonstrate its potential for sustainable agricultural applications in rural areas. This approach offers a cost-effective and environmentally friendly sustainable solution for irrigation, contributing to improving water and energy security.

Keywords: Renewable energy, Sustainable agriculture, Hybrid water pumping system, Nonlinear controls, Motor drive, Energy management system.

Received: 30th July 2025; Revised: 17th Sept 2025; Accepted: 28th Sept 2025; Available online: 2nd Oct 2025

1. Introduction

The intensive use of conventional electricity and diesel in the agricultural sector has significant environmental repercussions (Qin *et al.* 2024). Such practices contribute to greenhouse gas emissions, air pollution, and soil degradation. Furthermore, reliance on fossil energy sources, such as diesel fuel, exposes the agricultural sector to energy price volatility and elevated operating costs, particularly in remote rural areas. Considering these energy challenges, renewable energy sources are emerging as a viable alternative, offering sustainability, environmental friendliness, and long-term economic advantages (Udegbe *et al.* 2023). Given the escalating urgency of environmental challenges, adopting renewable energy is especially imperative in regions highly susceptible to climate impacts.

Recent studies have emphasized the critical importance of climate change mitigation and adaptation strategies in Mediterranean and semi-arid contexts. Simultaneously, the socio-economic prospects of the transition to renewable energy in rural and island regions have been explored. (Zafeiriou *et al.* 2022) highlight the socio-economic and environmental challenges associated with the energy transition in peripheral regions in the post-lignite era, highlighting the need for alternative energy sources and inclusive governance. This perspective further emphasizes the importance of integrating these sources, such as those proposed in this study, into regional development strategies to ensure both sustainability and societal acceptance. Furthermore, (Tampakis *et al.* 2017) demonstrate that public perceptions and behaviors regarding electricity consumption and renewable energy production are key determinants of the success of energy transitions, particularly in isolated or resource-constrained areas. Together, these studies support the argument that technical solutions must be aligned with socio-economic realities and public engagement to maximize their impact and transferability across various Mediterranean and semi-arid contexts. In North Africa, the effects of climate change are increasingly evident. Tunisia is experiencing more frequent and intense heatwaves, along with prolonged periods of drought. These climatic phenomena pose a significant threat to small-scale farmers. For instance, during the summer of 2021, Tunisia faced an exceptionally severe heatwave, with temperatures nearing 50°C. In the coming years, the Mediterranean region is expected to experience an increase in extreme weather events, including wildfires, floods, and prolonged droughts accompanied by rising aridity. Therefore, a transition to renewable energy is inevitable (IPCC 2021). Thanks to the development of the national wind atlas as illustrated in Fig.1 (a), Tunisia's wind map reveals several locations optimal for wind farm deployment. The most

*Corresponding author
Email: akramamriversailles@gmail.com (A.Amri)

https://doi.org/10.14710/ijre2025.61626
ISSN: 2252-4940/© 2025.The Author(s). Published by CBIORE

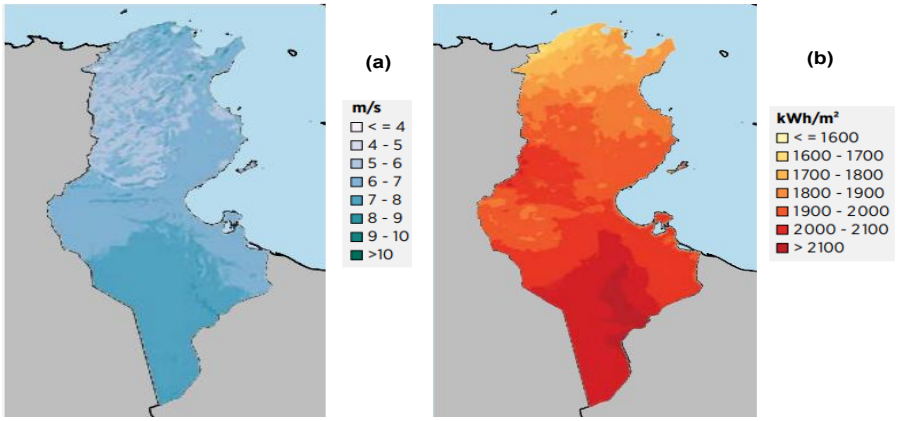

Fig.1. Renewable Energy Resources in Tunisia: (a) Wind Map, (b) Global Solar Radiation on a Horizontal Surface (Source: IRENA 2020)

promising sites, with wind speeds exceeding 7 m/s at a height of 80 m, are located in the regions of Bizerte and Nabeul, the central region (Kasserine, Sidi Bouzid), and the southern areas (Tataouine, Cap-Occidental, Gabès, and Kébili). In comparison, regions exhibiting less favorable wind conditions, where speeds range between 6.5 and 7 m/s, are found in the eastern part of Tozeur, the eastern coast of Médenine, and the Monastir region. The gross wind energy potential in Tunisia is estimated to exceed 8,000 MW (IRENA 2020). Concerning PV energy, as depicted in Fig.1(b), Tunisia benefits from over 3,000 h/y, although this parameter varies by region. Most southern provinces receive more than 3,200 hours of solar exposure annually, with peaks reaching 3,400 hours along the southern coast. In contrast, the Northern provinces experience a minimum sunshine duration ranging between 2,500 and 3,000 hours of equivalent full sun (IRENA 2020). Solar radiation levels range from approximately 1,800 kWh/m²/year in the north to 2,600 kWh/m²/year in the south. Global solar radiation on a horizontal surface serves as a reliable indicator for assessing the photovoltaic potential of a given site. The daily average of global solar radiation ranges between 4.2 kWh/m²/day in the northwestern of Tunisia, and 5.8 kWh/m²/day in the far south. In Tunisia, the annual yield of PV systems varies by region, ranging from around 1,450 kWh/kWp in the northwest to 1,830 kWh/kWp in the south easternmost areas. While most PV projects are geared toward the agricultural sector, a smaller share serves the industrial and service sectors. Furthermore, 64% of installed systems have a capacity below 100 kW, indicating a predominance of small-scale installations. (National Agency for Energy Conservation 2022).

Although renewable energy systems are gaining traction across multiple sectors, including agriculture, industry, and services, their impact is especially transformative in rural regions. In regions such as Sidi Bouzid, renewable energy not only presents a cost-effective alternative but also offers a sustainable and decentralized solution for vital needs such as irrigation and water pumping. The majority of these systems are powered by PV generators, which are particularly suitable for agricultural use during the summer months. This period corresponds with peak energy demand and the highest solar irradiance, allowing PV systems to operate at maximum efficiency and align perfectly with irrigation requirements (Saady *et al.* 2021; Mazzeo *et al.* 2021). During low sunlight or at night, the integration of PV systems with WTs offers a reliable hybrid solution that mitigates the intermittency of renewable sources, ensuring continuous power supply for agricultural applications (Al-Falahat *et al.* 2022).

In irrigation systems powered by WTs, which convert wind energy into mechanical power (Echiheb *et al.* 2025), the generated energy can either be used directly for water pumping or converted into electricity via an electric generator to drive a water pump. Such systems are compared with those powered by diesel engines and PV generators (Desta *et al.* 2023), based on real-world data, this study underscores the advantages of renewable energy technologies in reducing greenhouse gas emissions and lowering the energy costs associated with water pumping. Hence, a comparative analysis of various WT models and their performance across different installation sites is presented (Wong *et al.* 2018). The findings from this study confirm the suitability of WTs for irrigation-related pumping applications. To overcome the limitations posed by variable wind conditions, several studies have proposed integrating battery storage with wind energy systems. This approach ensures uninterrupted pump operation during periods of insufficient wind (Rehman and Sahin 2018). Additionally, the combined use of WTs and battery storage is further investigated through electrical simulations (Calderon *et al.* 2019), offering insights into system performance under diverse operational scenarios.

It has been documented that certain authors employ PV generators exclusively as the power supply source. (Cervera *et al.* 2020) propose an integrated model for estimating irrigation quality based on different meteorological data and demonstrate the results of applying the tool on site. A further study (Sharma *et al.* 2020) examines the strategies for overcoming various faults during the operation of the irrigation system. In (Barrueto *et al.* 2018), two categories of PV systems are examined for their suitability to the irrigation sector: those that are grid-connected and those that are stand-alone. Hence, the findings indicate that grid-connected systems exhibit superior performance in comparison to stand-alone systems, attributable to their enhanced reliability. The PV-based irrigation system with a water tank, using real data, is examined in (Shinde and Wandre 2015) as a potential means of expanding irrigated areas in the country. The results demonstrate the viability of such a system, even in locations characterized by relatively high latitude. In (Gabrovska *et al.* 2019), a PV system integrated with a battery is proposed for the purpose of powering a water pump during the irrigation period and for the storage of fruit during the remainder of the year. This approach is intended to enhance the utilization of the system on a year-round basis. Buildings on this concept, (Monís *et al.* 2020) introduce a sizing methodology for a PV system integrated with a water tank, optimized using genetic algorithms.

Hybrid Renewable Systems (HRS) that combine two or more energy sources, with or without storage components, have been extensively examined in the literature (Stoyanov *et al.* 2021), as shown in Fig.2. Among the various configurations of HRS, a case study in (Al-Ghussain *et al.* 2018) demonstrates that the integration of batteries not only enhances system reliability but also significantly reduces energy costs. Some researchers focus specifically on PV generators as the primary energy source. Other studies have explored strategies to improve the reliability of stand-alone irrigation systems (Ferrarese *et al.* 2024), with the most common approach involving the integration of a storage component (Chatterjee and Ghosh 2020). (Ahmed *et al.* 2025) present a comprehensive review of studies evaluating water tanks as a viable form of energy storage, highlighting both their operational simplicity and economic advantages. In (Saputra *et al.* 2018), the authors propose a hybrid system combining a WT and a PV generator for agricultural irrigation. Meanwhile, systems without storage have been analyzed in (Ronad and Jangamshetti 2015; Xiang *et al.* 2017; Powell *et al.* 2019), where findings indicate that WTs do not form part of the optimal configuration for irrigation systems. Similar research in (Campana *et al.* 2015) compares the performance of PV and WT powered systems. However, a study in (Vick and Neal 2012) reveals that both types of generators can contribute positively by increasing the volume of pumped water, depending on the system design and environmental conditions.

Pumping for irrigation is a sector that is both sensitive to climate variability and responsible for significant greenhouse gas emissions when it relies on diesel technologies. The transition to HWPS therefore serves a dual purpose: it contributes to mitigation by reducing the carbon footprint of water pumping for agricultural purposes, while strengthening adaptation by ensuring the reliability of irrigation during periods of drought or heat stress. Recent research illustrates these two complementary dimensions. (Nydrioti *et al.* 2024) analyzed urban water resource management in various climate scenarios in Mediterranean regions, highlighting the importance of integrated planning for adaptation. (Bozoudis *et al.* 2021) assessed the carbon footprint of transportation activities in a large Greek hospital, highlighting the value of detailed sectoral accounting for mitigation efforts. (Assimacopoulos *et al.* 2025) developed a national framework for monitoring and evaluating climate change adaptation in Greece, providing an institutional model for tracking the effectiveness of measures. Similarly, (Tsepi *et al.* 2024) broke down CO_2 emissions in Greece over two decades, demonstrating the complexity of the factors that determine mitigation challenges. By situating the present study within the context of this work, we show that the hybrid PV-WT pumping system not only offers an operationally viable solution for semi-arid agriculture but also contributes to the broader goals of low-carbon development and climate resilience.

HWPS have been extensively studied in the scientific literature. However, most existing research focuses on simplified system architectures and limited operational scenarios, often employing basic control strategies. These constraints limit the comprehensive evaluation of system performance under dynamic and real conditions. To overcome these limitations, the implementation of a dedicated EMS is essential, as it is responsible for optimizing system operation and reducing overall operational costs by balancing energy production from renewable sources with the power demands of electrical loads and storage units. Additionally, it protects storage components from overcharging and deep discharging, while enabling energy exchange with the grid when necessary. When coupled with an optimization algorithm, the EMS further improves power supply reliability and contributes to minimizing the cost of energy production (Poompavai and Kowsalya 2019). In addition, the selection of a motor for pumping in the HWPS requires a comprehensive evaluation of several criteria, including efficiency, reliability, cost and availability. This evaluation process involves the investigation and comparison of multiple motor types, each presenting distinct advantages and limitations. Choosing the most suitable motor is therefore essential to ensure optimal system performance and long-term operational sustainability. DC motors are widely adopted for their simplicity (Kumar 2020); however, their reliance on brushes and commutators results in frequent maintenance requirements. To overcome these limitations, brushless permanent magnet (BLDC) motors have been proposed as a viable alternative (Swan *et al.* 2010; Abdellahi *et al.* 2019). Nevertheless, their application is generally limited to low-power PV systems. Consequently, numerous researchers have investigated water pumping systems powered by AC motors, such as permanent magnet synchronous motors (PMSMs) and IMs.

Among these, IMs have exhibited superior performance thanks to their reliability and minimal maintenance requirements. Furthermore, based on their cost-effectiveness, IMs are commonly selected for irrigation and water pumping in developing countries (Elkholy and Fathy 2016). However, IMs inherently exhibit a coupling between torque and flux, which increases the complexity of their control. To address this challenge, several advanced control techniques have been proposed, including Field-Oriented Control (FOC), Sliding Mode Control (SMC), and Direct Torque Control (DTC) (Saady *et al.* 2021; Saady *et al.* 2023).

Nevertheless, some strategies, particularly FOC, are highly sensitive to parameter variations, especially changes in the rotor time constant, which can compromise performance. To overcome this limitation, an IOFL controller has been introduced (Mishra and Mohanty 2017). This method operates independently of assumptions regarding reference frame orientation, thereby enhancing robustness and control

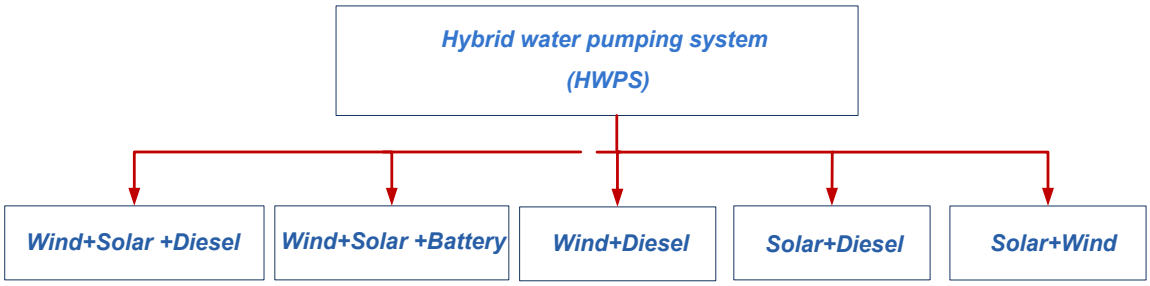

Fig 2. Classification of different types of HWPS

precision.

Expanding upon the previously discussed challenges and control strategies in HRS, this paper presents a theoretical study focused on the integration of power converters and appropriate control techniques to optimize water flow in a HWPS aligned with the climatic and agricultural conditions of the Sidi Bouzid region in Tunisia. A comprehensive system-level analysis was conducted to identify and configure the key components essential for ensuring reliable and high-performance operation. These include PV panels designed to deliver customized electrical output, a WT coupled with a DFIG for efficient wind energy conversion, dedicated power converters to manage and optimize energy flow, an IM to convert electrical energy into mechanical motion, and a centrifugal pump to provide stable and continuous water circulation aligned with crop irrigation needs. Accordingly, an EMS is proposed in this work and evaluated under various environmental conditions, including real-world fluctuations in wind speed and solar irradiance, to assess its adaptability and performance.

In addition to addressing Tunisia's urgent energy needs, this study makes a significant contribution in two aspects. First, it introduces a new hybrid water pumping system designed to operate without battery storage, an approach that reduces costs and ensures long-term sustainability. Second, although this research focuses on the semi-arid region of Sidi Bouzid in Tunisia, the methodology and findings are broadly transferable to other Mediterranean and semi-arid regions facing similar water and energy challenges.

The remainder of this article is organized as follows: Section 2 provides a detailed description of the proposed HWPS topology. Section 3 discusses the mathematical models that form the basis of HWPS. Section 4 covers the control algorithms implemented across the various system components, introduces the EMS flowchart, and describes the selected exploration scenarios. Section 5details the meteorological and environmental conditions that must be met to successfully conduct a HWPS simulation. Section 6 analyzes the simulation results based on the implemented control strategies and evaluates the overall performance of the system. Finally, section 7 summarizes the main conclusions and key contributions of this study.

2. Overview of the proposed HWPS design

The proposed HWPS, as illustrated in Fig.3, comprises three parts: wind energy generation using a WT-DFIG with rotor-side control; solar energy via PV panels with a boost converter and an inverter; and a load comprising an IM coupled to a centrifugal pump for irrigation. Control strategies include SMC and MPPT for the WT subsystem, MPPT for the PV subsystem, and IOFL for precise control of the IM. All converters are controlled by dedicated PWM techniques to meet their specific operational needs. An EMS ensures optimal operation under variable environmental conditions.

3. Mathematical Models of HWPS Main parts

3.1 Wind Energy Source Side

Wind systems convert kinetic wind energy into electricity using blades, a gearbox, and a generator that transforms rotational motion into electrical energy via magnetic interactions (Chhipą *et al.* 2022). Wind speed fluctuations are modeled using a specific mathematical expression presented as follows:

$$V(t) = \bar{V} + \sum_{i=1}^{7} k_i \sin(a_i \omega t) \quad (1)$$

Where:

$$\bar{V} = 8.2, \omega = \frac{2\pi}{10};\ k_1 = 2, k_2 = -1.75, k_3 = 1.5, k_4 = -1.25, k_5 = 1, k_6 = 0.5, k_7 = 0.25;\ a_1 = 1, a_2 = 3, a_3 = 5, a_4 = 10, a_5 = 20, a_6 = 50, a_7 = 100.$$

The expression of mechanical power generated by the WT system is given by equation (2) as follows:

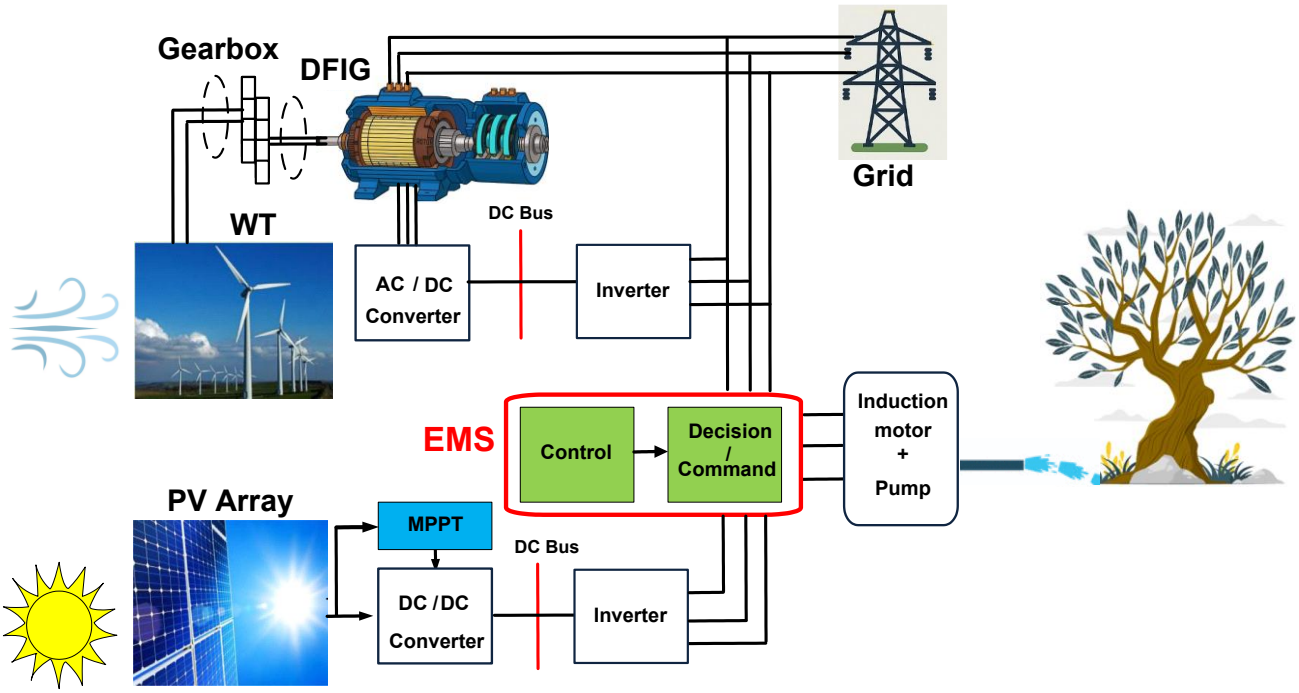

Fig 3. HWPS general overview

$$P_t = \frac{1}{2}\rho\pi R^2 V^3 C_p(\lambda,\beta) \quad (2)$$

In this study, the power coefficient $C_p(\lambda,\beta)$ is represented by the following equation (3):

$$C_p(\lambda,\beta) = c_1\left(c_2\left(\frac{1}{\lambda+0.08\beta} - \frac{0.035}{\beta^3+1}\right) - c_3\beta - c_4\right)e^{-c_5\left(\frac{1}{\lambda+0.08\beta} - \frac{0.035}{\beta^3+1}\right)} + c_5 \quad (3)$$

Where: c_1=0.5, c_2=116, c_3=0.4, c_4=5 and c_5=21.

Given that we're going to exploit the rotor side of the DFIG, the expression of the generated electrical power is expressed as follows (Btissam *et al.* 2021):

$$P_r = \frac{3}{2}(V_{rd}i_{rd} + V_{rq}i_{rq}) \quad (4)$$

3.2 PV Energy Source Side

3.2.1 Design of the PV Panel

PV systems convert sunlight into electrical energy through semiconductor materials in the solar cells. The generated direct current is then converted into alternative current via an inverter for use in specific applications. The system incorporates an MPPT algorithm to optimize energy capture under varying sunlight conditions. The expression of irradiance on inclined surface considered in this study is given by equation (5) (Zhang *et al.* 2024):

$$G = G_b.\cos(\theta) + G_d\frac{1+\cos(\beta)}{2} + G_r\frac{1-\cos(\beta)}{2} \quad (5)$$

The output current of the one-diode PV system is expressed as follows:

$$I_{pv} = n_p.I_{ph} - n_p.I_0\left(exp\left[\frac{V_{pv} + (R_s.n_s/n_p)I_{pv}}{V_t a}\right] - 1\right) - \frac{V_{pv} + (\frac{R_s.n_s}{n_p})I_{pv}}{R_p.n_s/n_p} \quad (6)$$

3.2.2. Design of Boost Converter

A DC-DC boost converter is a type of voltage regulator that is placed between a PV array and an inverter. It converts the input DC voltage V_{pv} to a higher DC voltage V_{dc} based on its duty cycle (α), which is controlled by the MPPT control. The boost output voltage and output current are calculated as follows:

$$V_{dc} = \frac{V_{pv}}{1-\alpha} \quad (7)$$

$$I_{dc} = I_{pv}(1-\alpha) \quad (8)$$

3.3 Pumping As System Load Side

This section focuses on the load subsystem, covering the IM and centrifugal pump used for irrigation. The mathematical model for the motor's dynamics such as speed, torque and flux control and the pump's power requirements is described.

Hence, the electrical equations in matrix form for voltages of the IM in the (d-q) frame are expressed by:

$$\begin{bmatrix}V_{rd}\\V_{rq}\end{bmatrix} = \begin{bmatrix}R_r & 0\\0 & R_r\end{bmatrix}.\begin{bmatrix}i_{rd}\\i_{rq}\end{bmatrix} + \frac{d}{dt}\begin{bmatrix}\phi_{rd}\\\phi_{rq}\end{bmatrix} + \begin{bmatrix}0 & -\omega\\\omega & 0\end{bmatrix}.\begin{bmatrix}\phi_{rd}\\\phi_{rq}\end{bmatrix} \quad (9)$$

$$\begin{bmatrix}V_{sd}\\V_{sq}\end{bmatrix} = \begin{bmatrix}R_s & 0\\0 & R_s\end{bmatrix}.\begin{bmatrix}i_{sd}\\i_{sq}\end{bmatrix} + \frac{d}{dt}\begin{bmatrix}\phi_{sd}\\\phi_{sq}\end{bmatrix} + \begin{bmatrix}0 & -\omega_s\\\omega_s & 0\end{bmatrix}.\begin{bmatrix}\phi_{sd}\\\phi_{sq}\end{bmatrix} \quad (10)$$

The stator and rotor fluxes in the (d-q) frame can be written as follows:

$$\begin{bmatrix}\phi_{sd}\\\phi_{sq}\end{bmatrix} = \begin{bmatrix}L_s & 0\\0 & L_s\end{bmatrix}.\begin{bmatrix}i_{sd}\\i_{sq}\end{bmatrix} + \begin{bmatrix}L_m & 0\\0 & L_m\end{bmatrix}.\begin{bmatrix}i_{rd}\\i_{rq}\end{bmatrix} \quad (11)$$

$$\begin{bmatrix}\phi_{rd}\\\phi_{rq}\end{bmatrix} = \begin{bmatrix}L_r & 0\\0 & L_r\end{bmatrix}.\begin{bmatrix}i_{rd}\\i_{rq}\end{bmatrix} + \begin{bmatrix}L_m & 0\\0 & L_m\end{bmatrix}.\begin{bmatrix}i_{sd}\\i_{sq}\end{bmatrix} \quad (12)$$

With $\omega = \omega_s - \omega_r$

A centrifugal pump operates by converting mechanical energy into hydraulic energy through centrifugal force. Known for its versatility, it is particularly efficient in handling large water volumes (Amri *et al.* 2025). The performance of this pump is characterized by several key parameters that are crucial for its evaluation. As shown in Equation 13, the load torque of the centrifugal pump is proportional to the IM speed square as follows:

$$T_{pump} = K_{pump}\Omega^2 \quad (13)$$

4. HWPS Control Strategies

This section outlines the control strategies implemented in the proposed system to ensure optimal operation. Two MPPT algorithms are employed to maximize energy extraction from both the WT and PV sources. The SMC technique is used to regulate the active and reactive power of the DFIG. The IM is controlled using IOFL to achieve stable operation for pumping purposes. Moreover, the EMS coordinates the energy flows between the renewable sources and the load, ensuring efficient system performance under different atmospheric conditions.

4.1. MPPT Algorithms for Source Side

The principle of an MPPT algorithm applied to a WT without speed control is based on extracting maximum power by acting solely on the power electronics, without active control of the speed of rotation i.e., no direct control of the generator or turbine. The objective is to maintain $\lambda = \lambda_{opt}$, where C_p is maximum (Peng *et al.,* 2024). For the PV source, the Incremental Conductance (INC) algorithm has been applied. This algorithm is based on the principle that the derivative of the output power with respect to the panel voltage equals zero at the maximum power point (Amri *et al.* 2025).

4.2. DFIG Rotor Side Controller

The DFIG is controlled by an SMC algorithm intended to drive the system state towards a defined sliding surface (Alami *et al.* 2022). This method ensures robust regulation of both active and reactive power via the rotor-side converter (Chojaa *et al.* 2021). The active and reactive power within the slip region is expressed by the following equation:

$$\begin{cases}S(P_s) = e_1 = P_{sref} - P_s\\S(Q_s) = e_2 = Q_{sref} - Q_s\end{cases} \quad (14)$$

The following equation expresses the derivative of this surface:

$$\begin{cases}\dot{e}_1 = \dot{P}_{sref} - \dot{P}_s \\ \dot{e}_2 = \dot{Q}_{sref} - \dot{Q}_s\end{cases} \quad (15)$$

After a detailed calculation of the surface and its derivative, we obtain the following expression:

$$\begin{cases}\dot{e}_1 = \dot{P}_{sref} + \frac{V_s L_m}{L_s}\left(\frac{V_{rqeq} + V_{rqn}}{L_r\sigma} - \frac{R_r + i_{rq}}{L_r\sigma} - \omega_r i_{rd} - \omega_r \frac{V_s L_m}{\sigma.\omega_s.L_r.L_s}\right) \\ \dot{e}_2 = \dot{Q}_{sref} + \frac{V_s L_m}{L_m}\left(\frac{V_{rdeq} + V_{rdn}}{L_r\sigma} - \frac{R_r + i_{rd}}{L_r\sigma} + \omega_r i_{rq}\right)\end{cases} \quad (16)$$

Consequently, the expression of the equivalent control and the stabilization control for active power are represented as follows:

$$\begin{cases}V_{rqeq} = \dot{P}_{sref}.\frac{\sigma.L_r.L_s}{V_s L_m} + R_r i_{rq} + \omega_r\sigma.L_r.i_{rd} + \omega_r \\ V_{rdn} = K_d.\mathrm{Sat}(e_1)\end{cases} \quad (17)$$

As well as for reactive power:

$$\begin{cases}V_{rdeq} = \dot{Q}_{sref}.\frac{-\sigma.L_s.L_r}{V_s L_m} + R_r i_{rd} - \omega_r\sigma.L_r.i_{rq} \\ V_{rqn} = K_q.\mathrm{Sat}(e_2)\end{cases} \quad (18)$$

Where:

$$\begin{cases}V_s = V_{sq} \\ \sigma = 1 - \frac{L_m^2}{L_r.L_s} \\ \omega_s - \omega_r = p\Omega_m\end{cases}$$

4.3. Load Side Controller

The IOFL strategy implementation facilitates the state feedback loop identification. This approach requires accurate measurements of the state vector, which are essential for converting a multi-input nonlinear control system into a linear and controllable system (Li *et al.* 2019b).

In this section, we propose to reformulate the IM model within the (*d,q*) reference frame. This method extends previous research and is based on equation (9) to equation (12).

$$\begin{cases}\dot{x} = f(x) + g(x).U \\ y = h(x)\end{cases} \quad (19)$$

Where$x = [x_1 \quad x_2 \quad x_3 \quad x_4]^T = [i_{sd} \quad i_{sq} \quad \phi_{rd} \quad \phi_{rq}]^T \in \mathrm{R}^n$ is the state vector, $U = \left[U_{sd} U_{sq}\right]^T \in \mathrm{R}^n$ the control input vector, y $\in \mathrm{R}^n$ is the output vector, *f(x)* and *g(x)* are *n* dimensional vector fields in the state space, *h(x)* is the scalar function of *x*.

$$f(x) = \begin{bmatrix}f_1(x) \\ f_2(x) \\ f_3(x) \\ f_4(x)\end{bmatrix} = \begin{bmatrix}-\gamma.i_{sd} + \delta.\eta.\phi_{rd} + \eta.p\omega.\phi_{rq} \\ -\gamma.i_{sq} - \eta.p\omega.\phi_{rd} + \delta.\eta.\phi_{rq} \\ \delta.L_m.i_{sd} - \delta.\phi_{rd} - p\omega.\phi_{rq} \\ \delta.L_m.i_{sq} - p\omega.\phi_{rd} - \delta.\phi_{rq}\end{bmatrix} \quad (20)$$

With:

$$\delta = \frac{R_r}{L_r} \quad ,\eta = \frac{L_m}{\sigma L_s L_r} \quad ,\gamma = \frac{L_m^2 R_r}{\sigma L_s L_r^2} + \frac{R_s}{\sigma.L_s} \quad ,\sigma = 1 - \frac{L_m^2}{L_s L_r}$$

$$g(x) = \begin{bmatrix}\frac{1}{\sigma.L_s} & 0 \\ 0 & \frac{1}{\sigma.L_s} \\ 0 & 0 \\ 0 & 0\end{bmatrix} \quad (21)$$

In order to control both the electromagnetic torque and the flux module square, the output vector is expressed as follows:

$$y = \begin{bmatrix}h_1(x) \\ h_2(x)\end{bmatrix} = \begin{bmatrix}\frac{1}{2}(\phi_{rd}^{\ 2} + \phi_{rq}^{\ 2}) \\ p\frac{3}{2}.\frac{L_m}{L_r}.(i_{sq}.\phi_{rd} - i_{sd}.\phi_{rq})\end{bmatrix} \quad (22)$$

Hence, the control system adjusts torque to regulate current demand, using the output's relative degree to derive a nonlinear control law governing system behaviour.

4.3.1 Relative Degree to the Output $h_1(x)$

The relative degree of $h_1(x)$ is expressed as follows:

$$\dot{h}_1(x) = L_f h_1(x) + L_g h_1(x).U = \dot{\phi}_{rd}.\phi_{rd} + \dot{\phi}_{rq}.\phi_{rq} \quad (23)$$

With $Lgh_1(x) = 0$. Note that the derivative of the first output does not involve the input U. This output must be derived a second time:

$$\ddot{h}_1(x) = L_f^2 h_1(x) + L_g L_f h_1(x).U.$$

After all the calculations, we obtain:

$$\begin{aligned}L_f^2 h_1(x) = {} & (\delta.\mathrm{L}_m)^2.(i_{sd}^2 + i_{sq}^2) + (\delta^2 + (\mathrm{p}.\omega)^2).\phi_{rd}^2 \\ & + (2\delta^2 + 2(\mathrm{p}.\omega)^2 + \delta^2\,\mathrm{L}_m.\eta).\phi_{rq}^2 \\ & - (\delta\ .\mathrm{L}_m + \delta^2.\mathrm{L}_m - 2.\gamma^2.\mathrm{L}_m)\mathrm{i}_{sd}\,\phi_{rd} \\ & + (8.p.\omega.\delta)\phi_{rd}\phi_{rq} - 3.p.\omega.\delta.L_m\,\mathrm{i}_{sq}\,\phi_{rd} \\ & - 2.p.\omega.\delta.L_m\,\mathrm{i}_{sd}\,\phi_{rq} \\ & - (\delta\ .\gamma.\mathrm{L}_m + \delta^2.\mathrm{L}_m + 2.\delta^2.\mathrm{L}_m)\mathrm{i}_{sq}\,\phi_{rq}\end{aligned} \quad (24)$$

$$L_g L_f h_1(x) = \left[\frac{L_m}{L_s}.\phi_{rd}\ \frac{L_m}{L_s}.\phi_{rq}\right] \quad (25)$$

The relative degree with respect to $h_1(x)$is $r_1=2$.

4.3.2 Relative degree to the output$h_2(x)$

The relative degree of $h_2(x)$ is given by:

$$\begin{aligned}&\dot{h}_2(x) = L_f h_2(x) + L_g h_2(x).U \\ &= \tfrac{3}{2}\tfrac{p.L_m}{L_r}\left[i_{sq}.\phi_{rd} + \dot{\phi}_{rd}.i_{sq} - i_{sd}.\phi_{rq} - \dot{\phi}_{rq}.i_{sd}\right]\end{aligned} \quad (26)$$

The development of calculus gives us:

$$\begin{aligned}&L_f h_2(x) = \frac{3}{2}p.\frac{L_m}{L_r}.[-\eta\,p\,\omega.(\phi_{rd}^2 + \phi_{rq}^2) \\ &+(\delta + \gamma)(i_{sd}.\phi_{rq} - i_{sq}.\phi_{rd}) \\ &+p\omega.(i_{sd}.\phi_{rd} - i_{sq}.\phi_{rq})]\end{aligned} \quad (27)$$

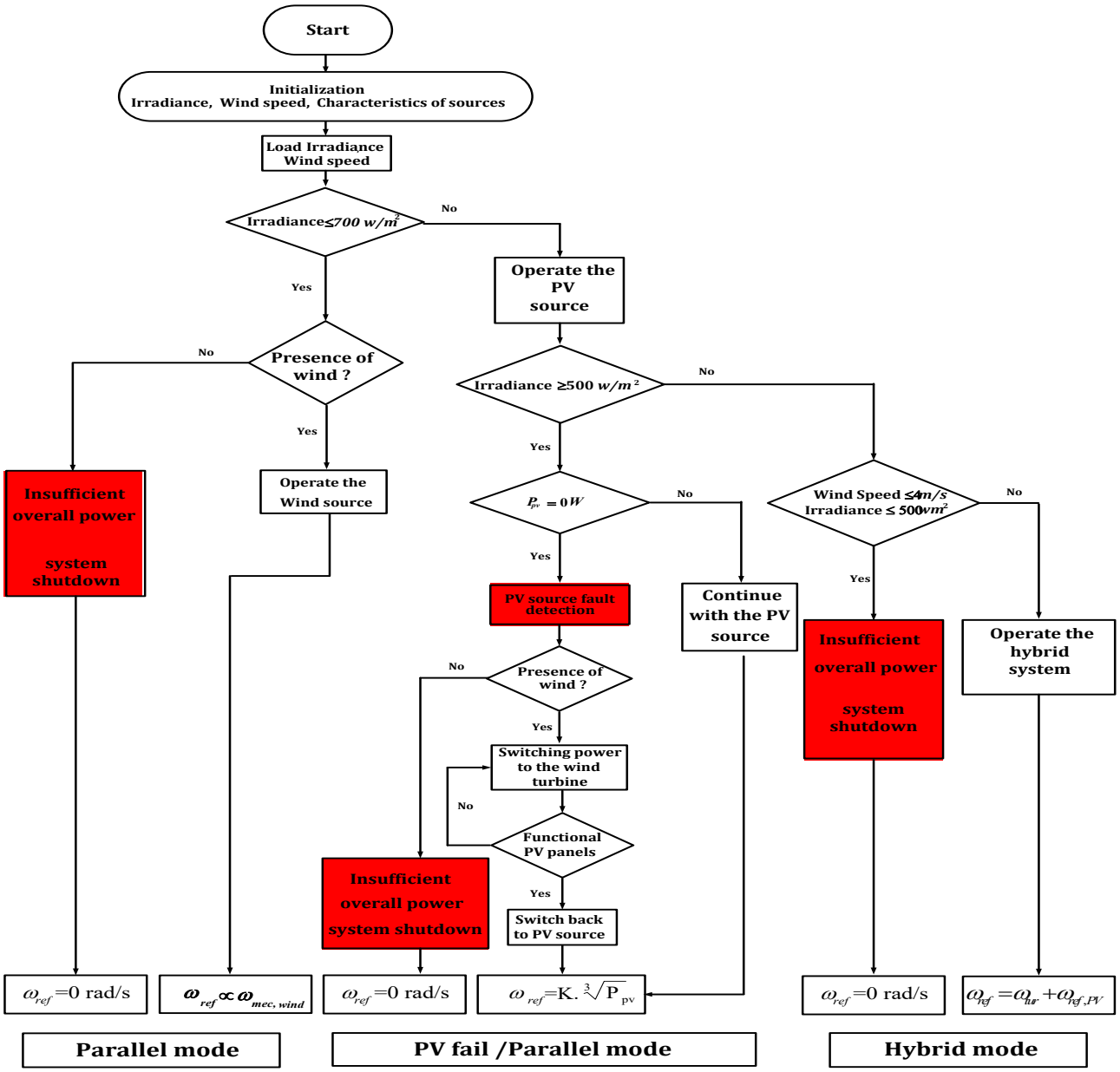

Fig 4. Flowchart of EMS

$$L_g h_2(x) = [-\frac{3}{2}p.\frac{L_m}{L_r}.\frac{1}{\sigma.L_s}.\phi_{rd}\ \frac{3}{2}p.\frac{L_m}{L_r}.\frac{1}{\sigma.L_s}.\phi_{rq}] \quad (28)$$

The relative degree with respect to $h_2(x)$ is r_2=2. So the relative degree of the overall system is $r = r_1 + r_2 = 3$ and is it less than that of the system (n=4) in the case where the system is partially linear and has an unobservable state. Considering only the output derivatives, we obtain:

$$\begin{bmatrix}\ddot{h}_1(x)\\ \dot{h}_1(x)\end{bmatrix} = \begin{bmatrix}L_f^2 h_1(x)\\ L_f h_2(x)\end{bmatrix} + E(x).\begin{bmatrix}U_{sd}\\ U_{sq}\end{bmatrix} \quad (29)$$

With:

$$E(x) = \begin{bmatrix}L_{g1}L_f h_1(x) & L_g L_f h_1(x)\\ L_{g1}h_2(x) & L_{g2}h_2(x)\end{bmatrix} = \frac{L_m}{L_s}.\begin{bmatrix}\phi_{rd} & \phi_{rq}\\ -\frac{3}{2}p\frac{1}{\sigma.L_r}.\phi_{rd} & \frac{3}{2}p\frac{1}{\sigma.L_r}.\phi_{rq}\end{bmatrix} \quad (30)$$

The non-linear control law is therefore given by:

$$\begin{bmatrix}U_{sd}\\ U_{sq}\end{bmatrix} = E^{-1}(x).\begin{bmatrix}-L_f^2 h_1(x)+v_1\\ -L_f h_2(x)+v_2\end{bmatrix} \quad (31)$$

If the determinant of the decoupling matrix is non-zero, the non-linear control law is defined by a relation that links the new

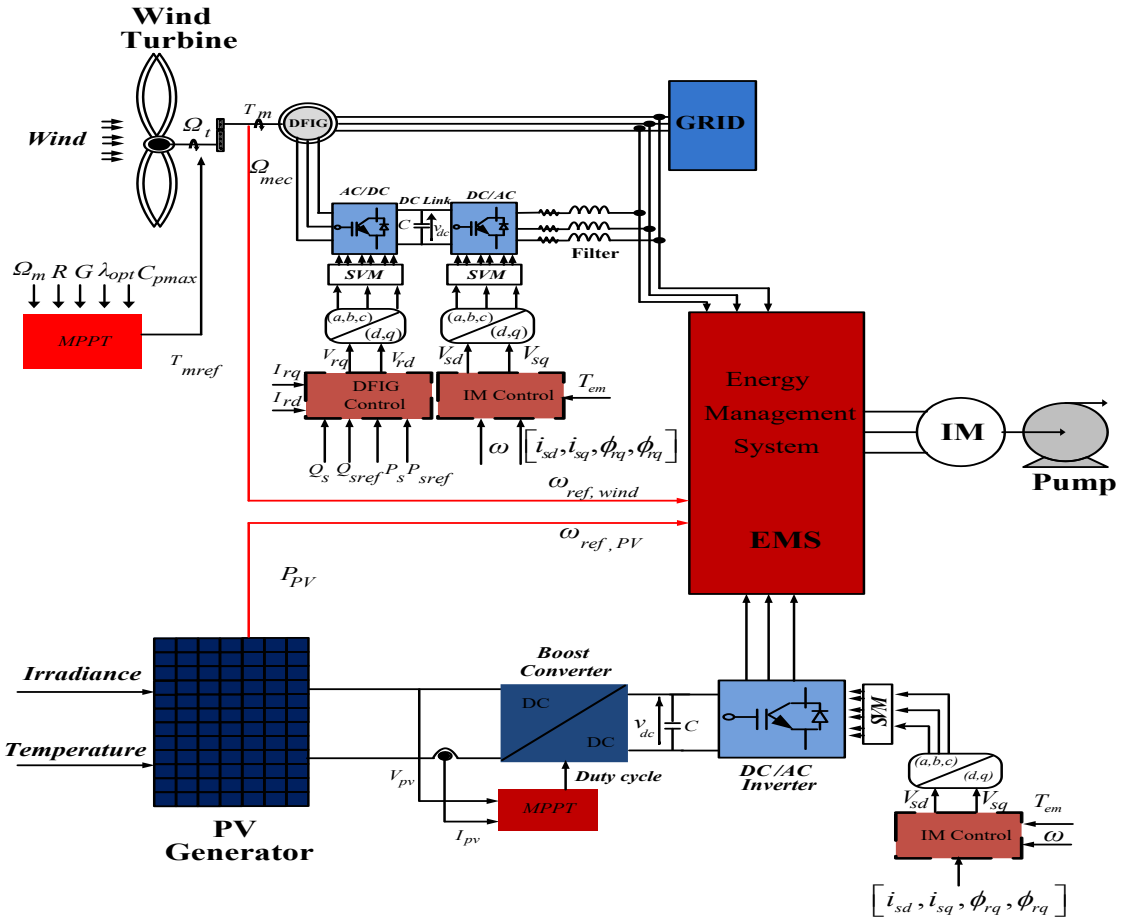

Fig 5. Synoptic diagram of the proposed HWPS

internal inputs *(v1, v2)* to the physical inputs (U_{sd}, U_{sq}). This command decouples the system so that:

$$\begin{cases} \ddot{h}_1(x) = v_1 = \ddot{y}_1 \\ \dot{h}_2(x) = v_2 = \dot{y}_2 \end{cases} \quad (32)$$

To ensure perfect regulation of flux and torque towards their respective references ϕ_{ref} and T_{ref}. Then, to effectively calculate the control, we write the desired differential equations (references) as follows:

$$\begin{cases} v_1 = \dot{\phi}_{ref} + \alpha_{11}(\dot{\phi}_{ref} - \dot{\phi}_r) + \alpha_{123}.(\phi_{ref} - \phi_r) \\ v_2 = \dot{T}_{eref} + \alpha_2.(T_{eref} - T_r) \end{cases} \quad (33)$$

4.4. Energy Management System Algorithm

After presenting the control strategies for managing the renewable energy sources and the pumping process in order to optimize the overall system performance, the HWPS integrates an EMS mechanism to efficiently coordinate the energy flows. The main challenge is ensuring reliable and uninterrupted water pumping, which requires optimizing the use of available renewable energy, minimizing losses, and maintaining system stability. Three operating scenarios are analyzed. The first involves parallel operation of both energy sources, while the second focuses on switching to the WT if the PV fails. The third scenario addresses the hybrid mode, where both sources collaborate to ensure continuous pumping during periods of low wind and irradiance. Fig.4 provides an overview of the implemented EMS algorithm, including the considered scenarios.

When the PV power is sufficient to operate the pump, the system progresses to the next step, where the IM speed is calculated based on the available PV power. If the latter is insufficient, the system then compares wind power. If the wind power meets the required demand, the WT is activated, and the IM speed is adjusted according to the mechanical speed of the WT. In cases where neither the PV nor the WT can supply the necessary power, the pump is deactivated. In the PV source failure case, the wind source can take over, provided that conditions are favorable. This process ensures continued operation by dynamically managing the priority between solar and wind energy. PV energy is preferred during periods of high irradiance, while wind energy is utilized when solar availability is low. The optimal integration of both sources ensures a consistent water flow. Moreover, the EMS is crucial for protecting system components by preventing sudden power fluctuations and ensuring seamless transitions between energy sources. By eliminating the need for battery storage, this approach reduces costs, enhances long-term sustainability, and improves the overall reliability of the pumping system.

Following a detailed description of the HWPS's components and the mathematical modeling of its control strategies, Fig.5 presents the overall system architecture.

5. Meteorological / Environmental Conditions for HWPS Simulation

As previously stated, the proposed HWPS is designed based on meteorological and environmental data collected from the Sidi Bouzid region of Tunisia (35.0381°N, 9.4858°E). As it is

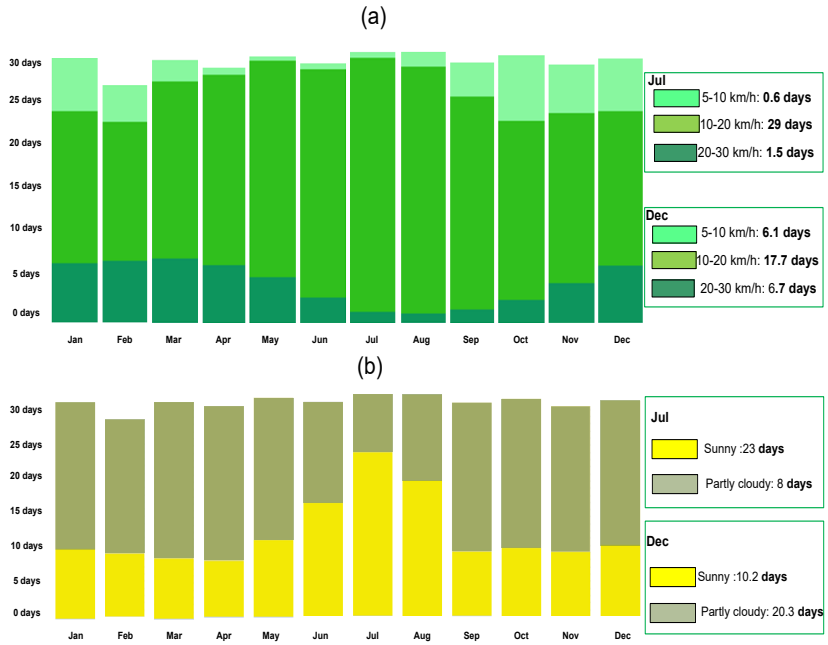

Fig 6. Characteristics of Sidi Bouzid region, Tunisia, for HWPS Simulation: (a) Wind speed distribution (days/month), (b) Cloudy and sunny day (source: meteoblue, 2023).

shown in Fig.6, which illustrates the seasonal variations in wind and solar resources, July is characterized by optimal solar and wind potential, while December is characterized by reduced availability.

This observation underscores the necessity for a hybrid energy approach. The region is characterized by a semi-arid climate, with hot summers (up to 36°C) and mild winters, and average rainfall of 200–300 mm, predominantly from October to March. The groundwater in Sidi Bouzid is located at a depth of 50–120 meters, with moderate salinity levels. To ensure sustainable irrigation, the implementation of powerful and well-designed pumping systems is essential.

6. Simulation Results

In this section, we presented the software architecture developed in Matlab/Simulink environment for the proposed HWPS. For the renewable energy sources, a 1.5 kW DFIG and a 1.6 kW PV system are considered. Meteorological data from the Sidi Bouzid region are applied as inputs for the wind and solar conversion systems. On the load side, a 1.5 kW induction motor is used to drive the centrifugal pump. To validate the system's performance, two cases are implemented. The first configuration tests the PV pumping chain without the EMS. This step is essential for analyzing and optimizing the system's static and dynamic responses, ensuring the pumping chain operates efficiently under specific conditions. By testing the system with PV source independently, we can isolate and evaluate the distinct contributions and limitations of solar energy, providing a clearer understanding of its individual effects on the system's overall efficiency and reliability. In the second configuration, the system is integrated with the EMS, and its performance is assessed under three distinct operating scenarios to account for different environmental conditions. This set allows for the coordination of energy flows between the renewable energy sources and the load, ensuring optimal system operation. By incorporating the EMS, it manages energy distribution, stabilizes fluctuations, and improves system efficiency, thereby testing the system's ability to handle dynamic changes in wind

Table1
Rated Quantities and Parameters of HWPS main parts

Parameters	Value	
	IM	**DFIG**
Rated Power	1.5kW	1.5Kw
Rated speed	1420 rpm	1420 rpm
Rated voltage	220/380 V	220/400 V
Number of pairs of poles	2	2
Rated current	3.1 A	6.1 A
Rated torque	10 N.m	10 N.m
Mutual inductance	L_m=0.258H	L_m=0.165H
Moment of inertia	J=0.031kg.m^2	J=0.031kg.m2
Stator resistance	R_s=4.850 Ω	R_s=1.75 Ω
Rotor resistance	R_r=3.805 Ω	R_r=1.68 Ω
Stator inductance	L_s =0.274H	L_s =0.295H
Rotor inductance	L_r =0.274H	L_r =0.104H
Viscous friction coefficient	f =0.008	f =0.002

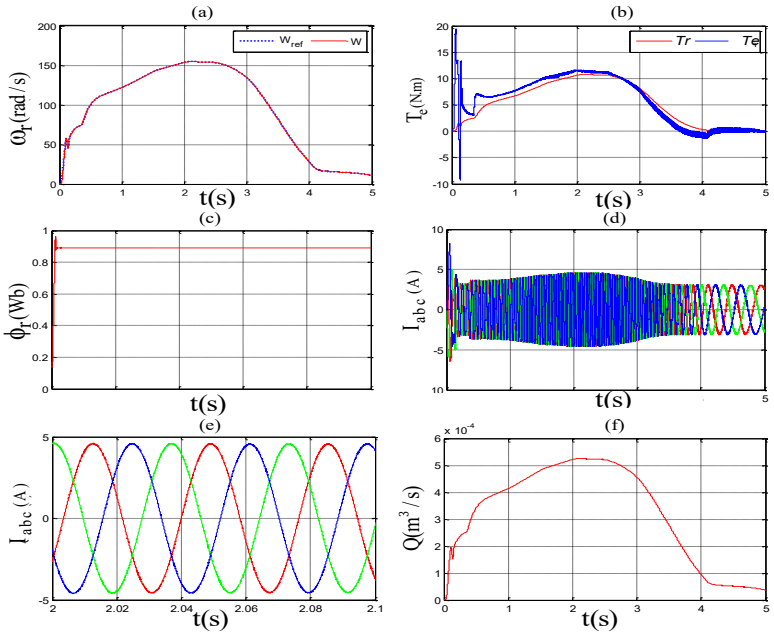

Fig 7. Simulation results from PV pumping system load side: (a) ω_r, ω_{ref}, (b) T_e,T_r, (c) ϕ_r, (d) I_{abc}, (e) zoom on I_{abc} (f) Q.

and solar availability. The parameters of the DFIG and the IM are summarized in Table 1.

The area of the farm under consideration is 2 hectares. In this project, the aim is to irrigate 120 olive trees for 10 hours a day, assuming that each olive tree requires around 120 Liters per day (at peak summer times in Tunisia). Therefore, the total volume of water required per day is: $Q_{required} = 4 \times 10^{-4} m^3/s$

6.1 Simulation Results of the PV pumping chain

The simulation was carried out to evaluate the performance of the PV water pumping system (PVWPS). Results from load are illustrated by Fig.7. By using the PV source for pumping, it is observed that the reference speed of the IM is determined as a function of the power generated by the PV array, as shown in Fig. 5. The simulation results, shown in Fig.7 (a), demonstrate that the rotor speed with the proposed IOFL control follows its reference values with remarkable accuracy. Fig.7 (b) illustrates the variation of the electromagnetic torque and the load torque of the IM during irradiation of the daily profile. The results indicate that the PVWPS equipped with the proposed IOFL control demonstrates a significant reduction in torque ripple. Moreover, under optimal power conditions, the electromagnetic torque converges toward its nominal value of 10 N.m, as reported in Table1. In this study, the load torque is assumed to be proportional to the rotational speed of the IM.

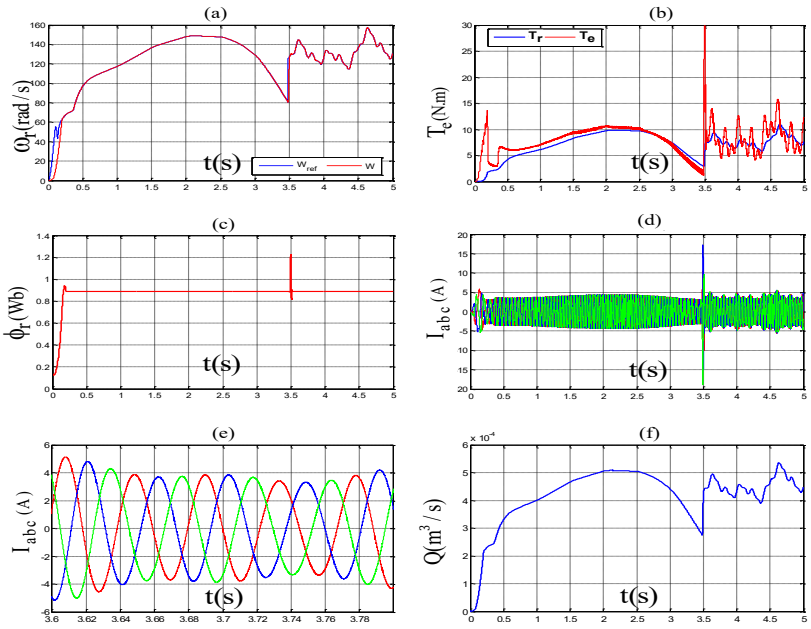

Fig 8. HWPS simulation results in parallel mode: (a) ω_r, ω_{ref}, (b) T_e,T_r, (c) ϕ_r, (d) I_{abc}, (e) zoom on I_{abc} (f) Q.

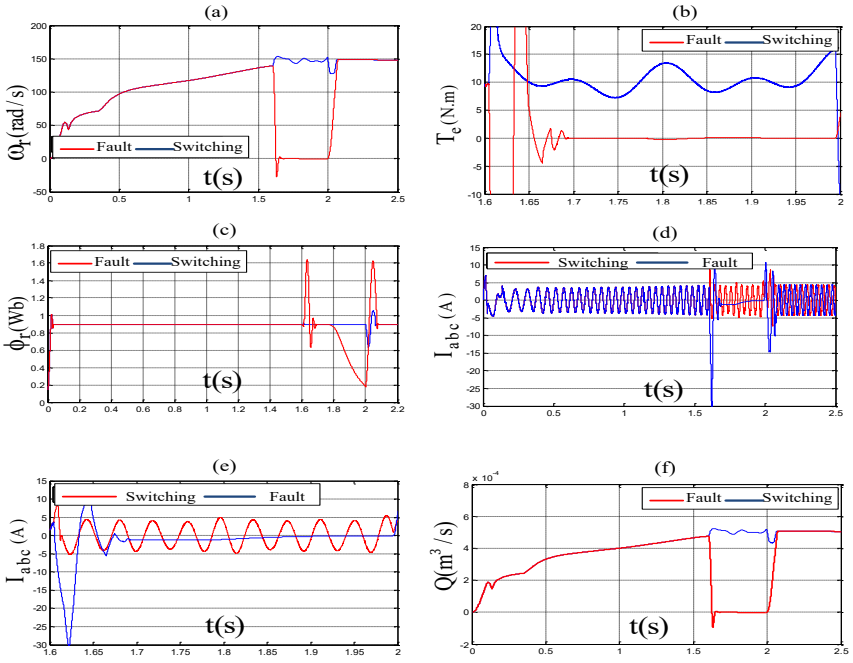

Fig 9.HWPS simulation results in PV defect mode: (a) ω_r, (b) T_e, (c) ϕ_r, (d) I_{abc}, (e) zoom on I_{abc} (f) Q.

Fig.7(c) shows the stator flux response, which follows its reference at 0.89 Wb. Fig.7 (d) and (e) illustrate the stator current using the IOFL control revealing that this current has an adequate and perfectly sinusoidal waveform. It is also observed that the stator currents increase with the intensity of solar irradiation. The evolution of the water flow rate is presented in Fig.7 (f). It is evident that this depends on the rotational speed of the IM and remains constant as long as the speed is stable. In this case study, it is observed that the flow rate drops below the required flow rate when the irradiance is below 700 W/m^2, causing a shortage of water for irrigation. Therefore, our approach of combining the WT and PV sources will be an alternative for continuous irrigation.

6.2 Simulation results of the HWPS using EMS

6.2.1 Simulation Results of the HWPS with Parallel Mode

The objective of this mode design is to simulate the interconnection of the PV and WT sources in order to analyze their performance and optimize their integration into the pumping chain. In this case study, the preferred solution in the hybrid system is to make PV energy the primary pumping source. In the event of failure or a significant reduction in irradiation, the WT serves as a backup option. This approach is illustrated in Fig.8, which illustrates the obtained results taking into account the flowchart depicted in Fig.4. Hence, Fig.8 (a) depicts the IM speed and its reference, Fig.8 (b) illustrates the IM electromagnetic torque, Fig.8(c) presents the flux of the IM, Fig.8 (d) and (e) show the IM current and a zoomed-in view of it, and while Fig.8 (d) illustrates the water flow. This scenario highlights the role of the EMS in ensuring fluid switching between energy sources for irrigation. When PV power decreases below a defined threshold (at t=3.5s), the system switches to WT, keeping IM speed and torque stable. Notably, water flow stabilizes between 4×10^{-4} and 5×10^{-4} m^3/s, thereby outperforming PV operation alone and ensuring reliable irrigation.

6.2.2 PV Defect Mode

This scenario illustrates the reaction of the HWPS to a loss of PV, in which the EMS switches to wind power, guaranteeing continuous pumping and stable water flow, as shown in Fig.9 which illustrates the HWPS reaction to PV fault and the critical role of the EMS. When the PV power falls at t =1.7s, the speed and torque of the IM briefly decrease before being stabilized by the WT. Magnetic flux and stator currents also exhibit transient fluctuations, which are rapidly corrected by the EMS intervention. More importantly, Fig.9(f) shows that despite the loss of PV, the EMS provides a stable water flow of around 5×10^{-4} m^3/s, allowing irrigation to continue without interruption. This confirms the EMS's effectiveness in accommodating energy source transitions while ensuring continuity and reliability of water pumping.

6.2.3 Energy Deficit Mode

This section assesses the performance of the EMS under energy deficit conditions and how it combines low solar and wind power inputs to maintain system performance, as illustrated in Fig.10. The simulation results underscore the HWPS's crucial role in maintaining system stability under energy deficit conditions. By coordinating the PV and WT inputs, the HWPS ensures a stable motor speed, adequate torque, and steady stator currents. This coordination allows continuous water flow to be maintained for irrigation, even when energy supplies are limited.

Simulation results confirm that the EMS-guided HWPS system provides stable, efficient irrigation despite the variability of renewable energies, proving its reliability for sustainable agriculture. When comparing the proposed hybrid system to other approaches described in the literature, several advantages become apparent. Irrigation systems that run solely on photovoltaic energy are often limited when there is little sunlight. Wind-powered systems offer interesting potential but are hindered by their intermittency. Hybrid systems with storage improve reliability but increase costs. In contrast, our

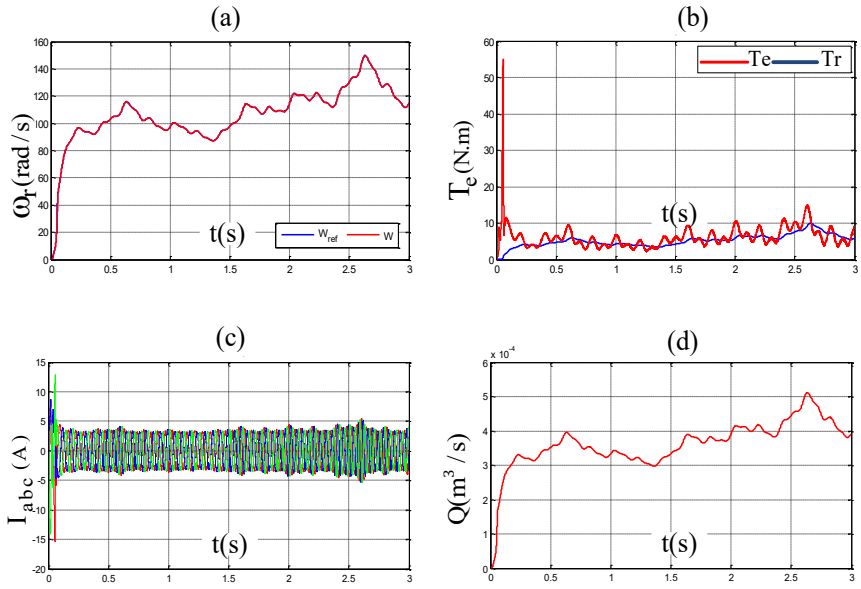

Fig 10. HWPS simulation results with energy deficiency (Hybrid Mode): (a) ω_r, ω_{ref}, (b) T_e,T_r, (c) I_{abc},(d) Q.

battery-free design ensures a reliable water supply at a lower cost.

7. Conclusion

This study allowed for the development, modelling, and evaluation of an HWPS adapted to sustainable agricultural irrigation in the semi-arid region of Sidi Bouzid, Tunisia. The system integrates MPPT, SMC, and IOFL controls into a dynamic EMS, providing stable operation without the need for battery storage. Simulation results confirm that the proposed configuration ensures reliable water supply, reduces costs, and improves energy efficiency compared to single-source or storage systems. Compared to PV-only solutions, which are limited during low solar irradiance, and WT-only systems, which suffer from resource intermittency, the proposed hybrid design offers superior reliability and economic feasibility. Similarly, unlike hybrid systems that rely on batteries, the current approach eliminates storage costs and maintenance charges. These results not only confirm the technical robustness of the proposed framework but also demonstrate its scalability and transferability to other Mediterranean and semi-arid regions.

8. Policy Implications

The implications of this study are clear for political decision-makers, particularly in the areas of energy transition, agricultural planning, and water resource management. First, the deployment of HWPS without batteries can reduce costs and promote decentralized energy access for agricultural producers, thereby reinforcing rural resilience. Second, by aligning irrigation practices with the availability of renewable energy, these systems can support national goals of reducing greenhouse gas emissions and promoting renewable energy strategies. Finally, this research highlights the importance of integrating renewable hybrid systems into agricultural policies and subsidies, particularly in regions where water scarcity and climate variability threaten food security.

Nomenclature

V	: Wind speed
P_t	: Mechanical power
Ω_t	: Turbine Speed
$C_p(\lambda,\beta)$	: Power coefficient
ρ, R	: Air density,Radius of the turbine
I_{rabc},I_{sabc}	: Rotor Current, Stator Current
V_{sd} , V_{sq}	: Stator Voltage in (d,q) reference
V_{rd} , V_{rq}	: Rotor Voltage in (d,q) reference
T_e	: Electromagnetictorque
ϕ_{sd}, ϕ_{sq}	: Stator Flux in (d,q) reference
ϕ_{rd}, ϕ_{rq}	: Rotor Flux in (d, q) reference
I_{sd},I_{sq}	: Stator Current in (d,q) reference
I_{rd},I_{rq}	: Rotor Current in (d ,q) reference
I_{ph}, I_0	: Photo-current, Saturation current
R_s , R_p	: Series resistance of the cell, parallel resistance of the cell
a, V_t	: Ideality factor of the diode ,thermical voltage
G_b ,G_d ,G_r	: Direct component (beam), Diffuse component, Reflected component (albedo)
G	: Total irradiance on the inclined surface
β	: Angle of the inclined surface to the horizontal
θ	: Incidence angle on an inclined surface
n_p,n_s	: Number of modules in parallel, Number of modules in series
V_{mpp},I_{mpp}	: Maximum voltage , current of the solar panel
k_{pump}	: Constant of the selected centrifugal pump.
P_r	: Rotor active power
ω_r	: Rotor speed
Q	: Water flow

Author Contributions: All authors have read and agreed to the published version of the manuscript.

Funding: The authors received no financial support for the research, authorship, and/or publication of this article.

Conflicts of Interest: The authors declare no conflict of interest.

References

Al-Ghussain, L., Ahmed, H., & Haneef, F. (2018). Optimization of hybrid PV–wind system: Case study Al-Tafilah cement factory, Jordan. *Sustainable Energy Technologies and Assessments, 30,* 24–36. https://doi.org/10.1016/j.seta.2018.08.008

Alami, H. E., Bossoufi, B., Motahhir, S., Alkhammash, E. H., Masud, M., Karim, M., Taoussi, M., Bouderbala, M., Lamnadi, M., & El

Mahfoud, M. (2022). FPGA in the loop implementation for observer sliding mode control of DFIG-generators for wind turbines. *Electronics, 11*(1), 116. https://doi.org/10.3390/electronics11010116

Amri, A., Moussa, I., & Khedher, A. (2025). Design and analysis of a photovoltaic water pumping system for sustainable agricultural irrigation. In *Proceedings of the 2025 IEEE 22nd International Multi-Conference on Systems, Signals & Devices (SSD)*, Monastir, Tunisia. IEEE. https://doi.org/10.1109/SSD64182.2025.10989905

Al-Falahat, A. M., Al-Nimr, M., Al-Mashaqbeh, I. A., Al-Dmour, N. A., & Al-Salaymeh, A. (2022). Energy performance and economics assessments of a photovoltaic-heat pump system. *Results in Engineering, 13,* 100324. https://doi.org/10.1016/j.rineng.2021.100324

Abdellahi, B., Mohamed Mahmoud, M. E. M., Dah, N. O., Diakité, A., El Hassen, A., & Ehssein, C. (2019). Monitoring the performance of a maximum power point tracking photovoltaic (MPPT PV) pumping system driven by a brushless direct current (BLDC) motor. *International Journal of Renewable Energy Development, 8*(2), 193–201. https://doi.org/10.14710/ijred.8.2.193-201

Assimacopoulos, D., Sebos, I., Chioti, D., & Katsiardi, P. (2025). Advancing climate change adaptation in Greece: Development and implementation of a national monitoring and evaluation system. *Euro-Mediterranean Journal for Environmental Integration*. https://doi.org/10.1007/s41207-025-00844-9

Ahmed, M. M., Bawayan, H. M., Enany, M. A., Elymany, M. M., & Shaier, A. A. (2025). Modern advancements of energy storage systems integrated with hybrid renewable energy sources for water pumping application. *Engineering Science and Technology, an International Journal, 62*, 101967. https://doi.org/10.1016/j.jestch.2025.101967

Barrueto Guzmán, A., Barraza Vicencio, R., Ardila-Rey, J. A., Núñez Ahumada, E., González Araya, A., & Arancibia Moreno, G. (2018). A cost-effective methodology for sizing solar PV systems for existing irrigation facilities in Chile. *Energies, 11*(7), 1853. https://doi.org/10.3390/en11071853

Bozoudis, V., & Sebos, I. (2021). The carbon footprint of transport activities of the 401 Military General Hospital of Athens. *Environmental Modeling & Assessment, 26*(2), 155–162. https://doi.org/10.1007/s10666-020-09701-1

Btissam, M., Douae, A., Yasmine, I., El B, C., Karim, M., & Bossoufi, B. (2021). Improvement of sliding mode power control applied to wind system based on doubly-fed induction generator. *International Journal of Power Electronics and Drive Systems (IJPEDS), 12*(1), 441–452. https://doi.org/10.11591/ijpeds.v12.i1.pp441-452

Campana, P. E., Li, H., & Yan, J. (2015). Techno-economic feasibility of the irrigation system for the grassland and farmland conservation in China: Photovoltaic vs. wind power water pumping. *Energy Conversion and Management, 103*, 311–320. https://doi.org/10.1016/j.enconman.2015.06.034

Calderon, J., Cureg, J., Diaz, M., Guzman, J., Rudd, C., & Le, H. T. (2019). Smart agriculture: An off-grid renewable energy system for farms using wind power and energy storage. In *Proceedings of the 2019 IEEE Power & Energy Society Innovative Smart Grid Technologies Conference (ISGT)* (pp. 1–5). Washington, DC, USA. https://doi.org/10.1109/ISGT.2019.8791576

Cervera-Gascó, J., Montero, J., del Castillo, A., Tarjuelo, J. M., & Moreno, M. A. (2020). EVASOR, an integrated model to manage complex irrigation systems energized by photovoltaic generators. *Agronomy, 10*(3), 331. https://doi.org/10.3390/agronomy10030331

Chatterjee, A., & Ghosh, S. (2020). PV based isolated irrigation system with its smart IoT control in remote Indian area. In *Proceedings of the 2020 International Conference on Computer, Electrical & Communication Engineering (ICCECE)* (pp. 1–5). Kolkata, India. https://doi.org/10.1109/ICCECE48148.2020.9223110

Chojaa, H., Derouich, A., Chehaidia, S., Zamzoum, O., & Elouatouat, M. (2021). Integral sliding mode control for DFIG based WECS with MPPT based on artificial neural network under a real wind profile. Energy Reports, 7, 4809–4824. https://doi.org/10.1016/j.egyr.2021.07.066

Chhipą, A. A., Chakrabarti, P., Bolshev, V., Chakrabarti, T., Samarin, G., Vasilyev, A. N., Ghosh, S., & Kudryavtsev, A. (2022). Modeling and control strategy of wind energy conversion system with grid-connected doubly-fed induction generator. *Energies, 15*(16), 6694. https://doi.org/10.3390/en15186694

Desta, M. A., Tibba, G. S., Issa, M. M., & Heyi, W. (2023). Performance and cost comparison of photovoltaic and diesel pumping systems in Central Rift Valley of Ethiopia. *Turkish Journal of Agricultural Engineering Research, 4*(1), 73–90. https://doi.org/10.46592/turkager.1272864

Echiheb, F., Majout, B., El Kafazi, I., Bossoufi, B., Rabhi, A., Bizon, N., Zhilenkov, A., & Mobayen, S. (2025). Experimental evaluation of an advanced predictive control technique for variable-speed wind turbine systems. *International Journal of Electrical Power & Energy Systems*. https://doi.org/10.1016/j.ijepes.2025.110668

Elkholy, M. M., & Fathy, A. (2016). Optimization of a PV fed water pumping system without storage based on teaching-learning-based optimization algorithm and artificial neural network. *Solar Energy, 139*, 199–212. https://doi.org/10.1016/j.solener.2016.09.022

Ferrarese, G., Pagano, A., Troiani, D., Ceni, A., Hutomo, A. I., Fontana, N., Marini, G., Mambretti, S., & Malavasi, S. (2024). Rethinking on-demand irrigation systems using IoT stand-alone technologies. *Engineering Proceedings, 69*, 77. https://doi.org/10.3390/engproc2024069077

Gabrovska-Evstatieva, K., Evstatiev, B., Trifonov, D., & Mihailov, N. (2019). Autonomous powering of an orchard irrigation system and fruit storage. In *Proceedings of the 47th International Symposium, Actual Tasks on Agricultural Engineering* (pp. 203–211). Opatija, Croatia.

IPCC. (2021). *Sixth assessment report – Working group 1: The physical science basis*. https://www.ipcc.ch/report/ar6/wg1/

IRENA. (2020). *Renewable capacity statistics 2020*. Abu Dhabi. https://www.mitigationmomentum.org/downloads/NAMA-proposal-for-renewable-energy-and-energy-efficiency-in-the-building-sector-in-Tunisia-December%202015.pdf

Kumar, S. (2020). Solar PV powered water pumping system using DC motor drive: A critical review. *International Journal of Trend in Research and Science, 5*(4), 1–8. https://doi.org/10.30780/IJTRS.V05.I04.001

Li, P., Zhang, J., Xu, R., Zhou, J., & Gao, Z. (2024). Integration of MPPT algorithms with spacecraft applications: Review, classification and future development outlook. *Energy*. https://doi.org/10.1016/j.energy.2024.132927

Li, P., Xiong, L., Wu, F., Ma, M., & Wang, J. (2019). Sliding mode controller based on feedback linearization for damping of sub-synchronous control interaction in DFIG-based wind power plants. *International Journal of Electrical Power & Energy Systems, 107*, 239–250. https://doi.org/10.1016/j.ijepes.2018.11.020

Mazzeo, D., Matera, N., De Luca, P., Baglivo, C., Congedo, P. M., & Oliveti, G. (2021). A literature review and statistical analysis of photovoltaic-wind hybrid renewable system research by considering the most relevant 550 articles: An upgradable matrix literature database. *Journal of Cleaner Production, 295*, 126070. https://doi.org/10.1016/j.jclepro.2021.126070

Monís, J. I., López-Luque, R., Reca, J., & Martínez, J. (2020). Multistage bounded evolutionary algorithm to optimize the design of sustainable photovoltaic (PV) pumping irrigation systems with storage. *Sustainability, 12*(3), 1026. https://doi.org/10.3390/su12031026

Mishra, R. N., & Mohanty, K. B. (2017). Implementation of feedback-linearization-modelled induction motor drive through an adaptive simplified neuro-fuzzy approach. *Sādhanā, 42*(12), 2113–2135. https://doi.org/10.1007/s12046-017-0741-6

National Agency for Energy Conservation. (n.d.). *ANME – National Agency for Energy Conservation*, from https://www.anme.tn/

Nydrioti, I., Sebos, I., Kitsara, G., & Assimacopoulos, D. (2024). Effective management of urban water resources under various climate scenarios in semiarid Mediterranean areas. *Scientific Reports, 14*(1), 28666. https://doi.org/10.1038/s41598-024-79938-3

Powell, J. W., Welsh, J. M., Pannell, D., & Kingwell, R. (2019). Can applying renewable energy for Australian sugarcane irrigation reduce energy cost and environmental impacts? A case study approach. *Journal of Cleaner Production, 240*, 118177. https://doi.org/10.1016/j.jclepro.2019.118177

Poompavai, T., & Kowsalya, M. (2019). Control and energy management strategies applied for solar photovoltaic and wind energy fed water pumping system: A review. *Renewable and Sustainable Energy Reviews, 107*, 108–122. https://doi.org/10.1016/j.rser.2019.02.023

Qin, J., Duan, W., Zou, S., Chen, Y., Huang, W., & Rosa, L. (2024). Global energy use and carbon emissions from irrigated agriculture. *Nature Communications, 15*, 3084. https://doi.org/10.1038/s41467-024-47383-5

Renewable Energy Solutions for the Mediterranean. (2016). *Country profiles: Tunisia*. Retrieved September 26, 2025, from https://www.res4med.org/wp-content/uploads/2017/11/Country-Profile-Tunisia-Report_05.12.2016.pdf

Rehman, S., & Sahin, A. Z. (2012). Wind power utilization for water pumping using small wind turbines in Saudi Arabia: A technoeconomical review. *Renewable and Sustainable Energy Reviews, 16*(6), 4470–4478. https://doi.org/10.1016/j.rser.2012.04.036

Ronad, B. F., & Jangamshetti, S. H. (2015). Optimal cost analysis of wind-solar hybrid system powered AC and DC irrigation pumps using HOMER. In *Proceedings of the 2015 International Conference on Renewable Energy Research and Applications (ICRERA)* (pp. 1038–1042). Palermo, Italy.

Saady, I., Karim, M., Bossoufi, B., Ouanjli, N., Motahhir, S., & Majout, B. (2023). Optimization and control of photovoltaic water pumping system using Kalman filter based MPPT and multilevel inverter fed DTC-IM. *Results in Engineering, 17*, 100829. https://doi.org/10.1016/j.rineng.2022.100829

Saady, I. I., Karim, M., Bossoufi, B., Motahhir, S., Adouairi, M. S., Majout, B., Lamnadi, M., Masud, M., & Al-Amri, J. F. (2021). Optimization for a photovoltaic pumping system using indirect field oriented control of induction motor. *Electronics, 10*(24), 3076. https://doi.org/10.3390/electronics10243076

Saady, I., Karim, M., Bossoufi, B., Motahhir, S., Adouairi, M. S., Majout, B., Lamnadi, M., Masud, M., & Al-Amri, J. F. (2021). Optimization for a photovoltaic pumping system using indirect field oriented control of induction motor. *Electronics, 10*(24), 3076. https://doi.org/10.3390/electronics10243076

Saputra, M., Syuhada, A., & Sary, R. (2018). Study of solar and wind energy using as water pump drive-land for agricultural irrigation. In *Proceedings of the 2018 4th International Conference on Science and Technology (ICST)* (pp. 1–4). Yogyakarta, Indonesia.

Sharma, V., Hossain, M. J., Ali, S. M. N., & Kashif, M. (2020). A photovoltaic-fed Z-source inverter motor drive with fault-tolerant capability for rural irrigation. *Energies, 13*(18), 4630. https://doi.org/10.3390/en13184630

Shinde, V. B., & Wandre, S. S. (2015). Solar photovoltaic water pumping system for irrigation: A review. *African Journal of Agricultural Research, 10*(20), 2267–2273. https://doi.org/10.5897/AJAR2015.9879

Stoyanov, L., Bachev, I., Zarkov, Z., Lazarov, V., & Notton, G. (2021). Multivariate analysis of a wind–PV-based water pumping hybrid system for irrigation purposes. *Energies, 14*(11), 3231. https://doi.org/10.3390/en14113231

Swan, L. G., & Allen, P. L. (2010). Integrated solar pump design incorporating a brushless DC motor for use in a solar heating system. *Renewable Energy, 35*(9), 2015–2026. https://doi.org/10.1016/j.renene.2010.02.002

Tampakis, S., Arabatzis, G., Tsantopoulos, G., & Rerras, I. (2017). Citizens' views on electricity use, savings and production from renewable energy sources: A case study from a Greek island. *Renewable and Sustainable Energy Reviews, 79*, 39–49. https://doi.org/10.1016/j.rser.2017.05.036

Tsepi, E., Sebos, I., & Kyriakopoulos, G. L. (2024). Decomposition analysis of CO_2 emissions in Greece from 1996 to 2020. *Strategic Planning for Energy & the Environment, 43*(3), 517–544. https://doi.org/10.13052/spee1048-5236.4332

Udegbe, S., Agupugo, O., Oyeniran, A., & Iyede, E. (2023). Environmental impact of modern agricultural practices: Strategies for reducing carbon footprint and promoting conservation. *International Journal of Management & Entrepreneurship Research, 4*(1), 73–90. https://www.fepbl.com/index.php/ijmer/article/view/1581

Vick, B. D., & Neal, B. A. (2012). Analysis of off-grid hybrid wind turbine/solar PV water pumping systems. *Solar Energy, 86*(5), 1197–1207. https://doi.org/10.1016/j.solener.2012.01.012

Wong, K. H., Chong, W. T., Poh, S. C., Shiah, Y.-C., Sukiman, N. L., & Wang, C.-T. (2018). 3D CFD simulation and parametric study of a flat plate deflector for vertical axis wind turbine. *Renewable Energy, 129*, 32–55. https://doi.org/10.1016/j.renene.2018.05.085

Xiang, C., Liu, J., Yu, Y., Shao, W., Mei, C., & Xia, L. (2017). Feasibility assessment of renewable energies for cassava irrigation in China. *Energy Procedia, 142*, 17–22. https://doi.org/10.1016/j.egypro.2017.12.004

Zafeiriou, E., Spinthiropoulos, K., Tsanaktsidis, C., Garefalakis, S., Panitsidis, K., Garefalakis, A., & Arabatzis, G. (2022). Energy and mineral resources exploitation in the delignitization era: The case of Greek peripheries. *Energies, 15*(13), 4732. https://doi.org/10.3390/en15134732

Zhang, T., Stackhouse, P. W., Macpherson, B., & Mikovitz, J. C. (2024). A CERES-based dataset of hourly DNI, DHI and global tilted irradiance (GTI) on equatorward tilted surfaces: Derivation and comparison with the ground-based BSRN data. *Solar Energy, 274*, 112538. https://doi.org/10.1016/j.solener.2024.112538